Tr. J. of Physics
22 (1998) , 611 – 619.

International Workshop on Linac-Ring
Type ep and γp Colliders

Some physical problems for photon colliders

Ilya F. GINZBURG
Institute of Mathematics,
630090 Novosibirsk - RUSSIA
E-mail: ginzburg@math.nsc.ru

Abstract

Higgs hunting at different colliders is discussed with new possibilities related to photon colliders are discussed. Brief review of discovery potential for new physics is presented.

1. Photon colliders

It is clear now that future linear colliders should be $e^+e^-/\ e\gamma/\ \gamma\gamma$ complexes. The γe and $\gamma\gamma$ components are *photon colliders* with the following main features [1],[2]:

- Characteristic photon energy $E_\gamma \approx 0.8E$ (E is the energy of electron in the basic e^+e^- collider.
- Mean energy spread $\frac{<\Delta E_\gamma}{E_\gamma} > \approx 0.1$.
- Photons will be polarized with mean helicity $<\lambda_\gamma> \approx 0.95$.
- This circular polarization can be transformed into linear one almost entirely without loss of quality of energy spectrum [3].
- The expected annual luminosity is $\mathcal{L}_b = 10 \div 30\ \mathrm{fb}^{-1}$ at the first stage with $2E = 0.5$ TeV [2].
- There are no special reasons against observations at small angles except technical details of design.
- One can organize *nonmonochromatic* variant of energy spectrum with $\mathcal{L}_n \approx 3\mathcal{L}_b$. One can prepare *supermonochromatic* variant with $<\Delta E_\gamma/E_\gamma> \approx 0.02$, $E_\gamma \approx 0.95E$, but with $\mathcal{L}_s \sim 0.1\mathcal{L}_b$.

2. Higgs boson at different colliders

Higgs boson is very important detail of Standard Model. It is responsible here for the observed breaking of the basic $SU(2)\,X\,U(1)$ symmetry and the generation of particle masses. Until Higgs boson discovery we cannot believe that SM is really the theory of our world.

The construction of SM is compatible with different variants of Higgs sector. Before symmetry breaking Higgs fields can be a number of isotopic doublets, triplets etc. For example, minimal Higgs sector in SUSY consists of 2 doublets. After symmetry breaking Higgs sector in 2–doublet model consist of two neutral Higgs bosons, one neutral axial boson and two charged Higgses. There is large field of opportunities here. Below we discuss the minimal variant of SM — **the standard Higgs of SM is an isotopic doublet**.

Main problems for HIGGS BOSON

1. To discover something and to measure its mass.
2. To test spin.
3. To test parity.
4. To test couplings with different particles — to verify Higgs mechanism of mass origin.
5. To measure Higgs total width Γ_{tot}.
6. To measure Higgs two photon width $\Gamma_{\gamma\gamma}$ – the counter for particles of SM that are heavier than Higgs.

The simultaneous using of results obtained at different colliders will give most of these properties [4]. Nevertheless, the results obtained at some single collider are preferable since the influence of systematical inaccuracies here can be reduced much more strong. In this respect, it is useful to compare

The potential of different colliders for above problems

problem	Tevatron /LHC	e^+e^- linear collider	Photon collider	$\mu^+\mu^-$ collider
Discovery	+	+	+ ($M_H \leq 400$ GeV)	+ ($M_H > 400$ GeV)
Mass	+	+	+	The best
Γ_{tot}	Poor	Poor	At $M_H > 200$ GeV	The best
Spin	Poor	Poor	+	+
Parity	—	—	The best*	+
$\Gamma_{\gamma\gamma}$	Poor	—	The best	—

* With Kotkin—Serbo mechanism [3] for variation of polarization.

If the Higgs boson mass M_H is larger than $2M_Z$, it can be discovered at LHC, photon colliders [1] or e^+e^- linear colliders [2] via the sizable decay mode $H \to ZZ$. For all types of collisions a background to this decay mode is rather small. If $M_H < 145$ GeV the Higgs boson can be discovered at e^+e^- linear colliders or photon colliders via the dominant decay mode $H \to b\bar{b}$ and at LHC – via the decay mode $H \to \gamma\gamma$.

The mass range $M_H = 140 - 190$ GeV is the most difficult one for the Higgs boson discovery. In this mass range the decay mode $H \to W^+W^-$ with real or virtual W's $(W^* \to q\bar{q}, e\bar{\nu}, ...)$ is dominant, branching ratios of other decay modes decrease rapidly and their using for the Higgs boson discovery is very difficult. The use of the $H \to W^+W^-$ decay at e^+e^- collider is also difficult due to a strong nonresonant W^+W^- background. The Higgs boson with the mass $M_H = 140 - 190$ GeV can be discovered at the photon collider via the $H \to W^+W^-$ decay mode [6].

3. Higgs boson with mass 140—190 GeV at photon collider

We considered both resonant $\gamma\gamma \to H \to W^+W^-$ and nonresonant QED contributions into this process:

$$d\sigma \propto |\mathcal{M}|^2 \equiv |\mathcal{M}^0|^2 + 2Re(\mathcal{M}^{0*}\mathcal{M}^H) + |\mathcal{M}^H|^2. \quad (1)$$

Here $|\mathcal{M}^0|^2$ stands for the background QED process $\gamma\gamma \to W^+W^-$, $|\mathcal{M}^H|^2$ is the contribution of $\gamma\gamma \to H \to W^+W^-$ and $2Re(\mathcal{M}^{0*}\mathcal{M}^H)$ describes the interference effect of these two mechanism. We use considerations of ref. [7] related to visible interference effect in this reaction as a starting point.

The WW production cross section at $140 < M_{WW} < 190$ GeV.

We consider initial photon state with total helicity zero (helicities of colliding photons $\lambda_1 = \lambda_2 = \pm 1$). Only such photon states can produce the Higgs boson. Helicity amplitudes for the nonresonant process (in the Born approximation) for such initial state are presented in ref. [9]. The amplitude $\mathcal{M}^H$ is written in the standard form via the well known amplitude of Higgs boson two photon decay [8].

In practice, we deal with the production of four fermions in the final state produced via intermediate W boson state. The distribution in invariant masses for such final state has a maximum at M_W with the width Γ_W and long tails away from the maximum. It describes by the well known Breit–Wigner spectral density for the W boson. One can view this as the production of W^* — a virtual W boson with the mass not equal to M_W. Because of this, the cross section does not vanish below the nominal threshold $M_{WW}^{thr} = 2M_W$. The most important effect comes from the corresponding modification in the final phase space [5]. It can be described via replacement of the relative velocity of W bosons in the center of mass frame entering final phase space

$$\beta = \frac{1}{s}\sqrt{(s - s_1 - s_2)^2 - 4s_1s_2}$$

by its convolution with above spectral density for the W boson $\varrho(M^2)$:

$$\beta \to \tilde{\beta} = \int ds_1 ds_2 \ \varrho(s_1) \ \varrho(s_2) \ \beta(s, s_1, s_2) \ \theta(s_1) \ \theta(s_2) \ \theta(\sqrt{s} - \sqrt{s_1} - \sqrt{s_2}).$$

Close to the threshold the $\gamma\gamma \to W^+W^-$ cross section can be approximated as:

$$\sigma \propto |\mathcal{M}|^2_{s=4M_W^2} \ \beta \ \Rightarrow |\mathcal{M}|^2_{s=4M_W^2} \ \tilde{\beta}.$$

The first of these equations relates to the stable W's, the second one takes into account effect of finite width. The accuracy of this approximation is about 30 % in whole mass interval considered. Note, that the Higgs boson width itself decreases by a factor of 20 for $M_H = 140$ GeV in comparison with its value at $M_H = 160$ GeV, so one can conclude that our approximation works well.

In our numerical estimates we integrated over production angle in the center of mass frame within the range $20° < \theta < 160°$. In Fig. 1 we show $\gamma\gamma \to W^+W^-$ cross section for various M_H as a function of the invariant mass M_{WW} of the W^+W^- pair for the initial state with total helicity zero. For $M_H \geq 180$ GeV the two–peak behavior observed in [7] is seen clearly. The interference term in eq. (1) is large for such Higgs boson masses. The height of the peak grows with decrease in M_H but its width ($\approx \Gamma_H$) becomes smaller and smaller.

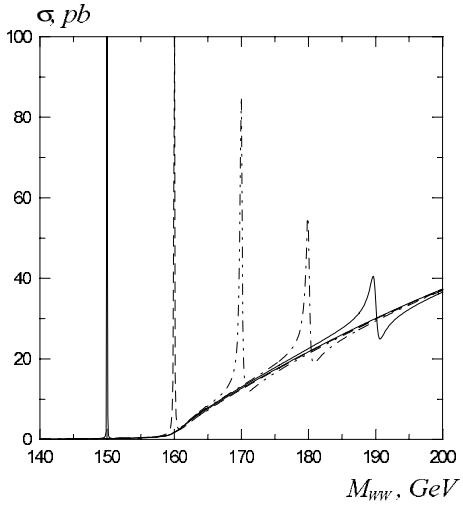

Figure 1. The $\gamma\gamma \to WW$ cross section for different M_H

With subsequent decrease in M_H, the background QED process is suppressed by the phase space and the interference also becomes small in comparison with the Higgs boson contribution.

The "experimental" cross sections.

After averaging over initial energy distribution of the photons, the Higgs boson signal decreases and seems to be hardly observable. To circumvent this problem, the observation of W bosons in the final state is mandatory (perhaps, via quark jets). In order to account for a finite resolution in M_{WW}, we consider a "smeared" cross section, similar to [7]:

$$\frac{d\sigma}{dM_{WW}^{meas}} = \int \frac{dM_{WW}}{\sqrt{2\pi}\, d} \exp\left[-\frac{(M_{WW}^{meas} - M_{WW})^2}{2d^2}\right] \frac{d\sigma}{dM_{WW}} \qquad (2)$$

The results for $d = 5$ GeV are shown[1] in Fig. 2 (above the nominal threshold), in Fig. 3 (below the nominal threshold) and in the Table.

In view of a very high degree of photon polarization expected at photon colliders, we present the Figures for completely polarized photon beams: $<\lambda_1>=<\lambda_2>=\pm 1$. Higgs boson signal deteriorates when $<\lambda_1><\lambda_2>$ decreases. Some result for $<\lambda_i>\neq 1$ are presented in the Table for "realistic mean helicities of the photons.

Higgs boson mass M_H, GeV	Characteristic M_{WW}, GeV	$<\lambda>$	σ^{bkgd}, pb	σ^{tot}, pb	$\frac{\sigma^{tot}-\sigma^{bkgd}}{\sigma^{bkgd}}$
140	140	1.0	0.11	0.98	8.0
		0.9	0.17	0.96	4.6
150	150	1.0	0.42	2.10	4.0
		0.9	0.60	2.13	2.6
160	159.7	1.0	3.65	6.81	87%
		0.9	4.86	7.74	59%
170	169.3	1.0	12.6	15.5	23%
		0.9	16.0	18.5	16%
180	178.5	1.0	21.8	23.7	8.7%
		0.9	25.3	27.0	6.7%
190	185	1.0	26.0	27.0	3.8%
		0.9	29.9	30.8	3.0%
	200	1.0	37.3	36.5	-2.1%
		0.9	40.2	39.4	-2.0%

Table 1. $\gamma\gamma \to W^+W^-$ cross sections for various M_H and $<\lambda>$

Above the nominal threshold the curves in Fig. 2 exhibit a characteristic shape. A deviation from the QED background is very sensitive to the presence of the Higgs boson. Therefore, such behavior of the experimental curve can be considered as an evidence for

[1]Let us stress that we do not perform any convolution with initial photon spectra. It is because of the fact that the real form of these effective spectra strongly depends on the details of the conversion design. Note also, that it can not be obtained by a simple convolution of individual spectra [1]. Real energy distribution of colliding photons should be measured for every energy of collider.

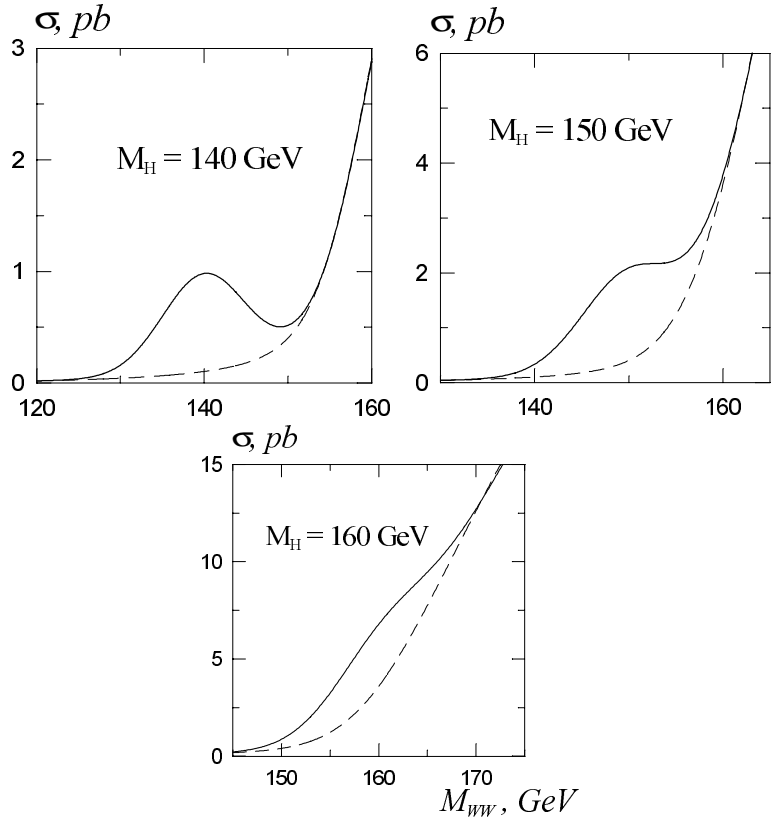

Figure 2. Smeared cross sections below the threshold. Dashed lines - nonresonant background.

the existence of the Higgs boson in this mass region. Here the background QED cross section varies from 3.6 pb for $M_{WW} = 160$ GeV to 30 pb for $M_{WW} = 190$ GeV. The Higgs boson production cross section adds another 3 pb for $M_H = 160$ GeV (87%). For $M_H = 190$ GeV an interference term in eq. (1) delivers 1.8 pb (6%) to the total cross section.

Below the threshold Higgs boson is observed even more clearly (Fig. 3). The averaged total cross section is about 1 pb in the whole region. It is larger than the cross section for the background process by almost a factor of 2 for $M_H = 160$ GeV and by a factor of 9 for $M_H = 140$ GeV.

This behavior is not surprising. The total Higgs boson production cross section averaged over the range of M_{WW} larger than the total width of the Higgs boson is equal to $\sigma_{\gamma\gamma\to H} = 4\pi^2\Gamma_{\gamma\gamma}/M_H^3$. The Higgs boson width drops out in this result. Roughly speaking, the cross section is almost independent of M_H in the considered mass range. At the

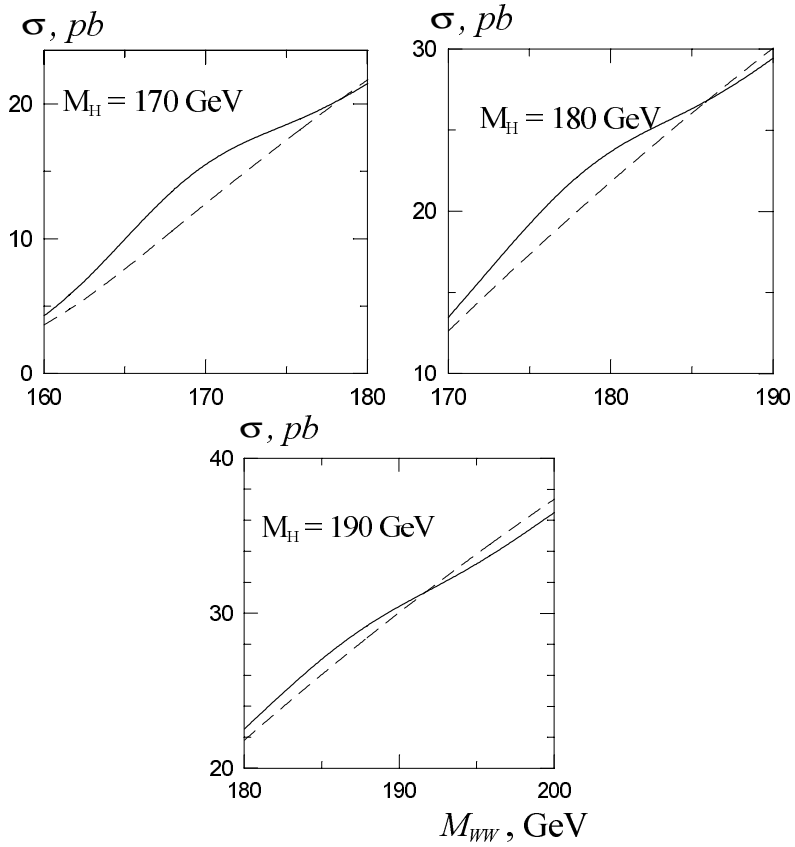

Figure 3. Smeared cross sections above the threshold. Dashed lines - nonresonant background.

same time, down to $M_H = 145$ GeV the W^+W^- decay mode still remains dominant. On the other hand, the QED background decreases fast with decrease in M_{WW} in the considered mass range. For this reason the two peak behavior, observed for $M_H > 180$ GeV, changes to a single resonance peak near and below the threshold and the Higgs boson signal becomes dominant in this region.

3.1. Conclusion

- Higgs boson with the mass $M_H = 140 - 190$ GeV can be observed and studied in the process $\gamma\gamma \to W^+W^-$ at future $\gamma\gamma$ colliders by measuring the invariant mass of produced W^+W^- system with reasonable resolution. A luminosity integral required for this observation is ~ 1 fb^{-1}.

- For $M_H \leq 160$ GeV the effect of the Higgs boson is still seen after being smeared over 15 GeV. This means that the signal of the Higgs boson lighter than 160 GeV can be observed even in the total $\gamma\gamma \to W^+W^-$ cross section without restrictions on the W^+W^- invariant mass.

- Similar calculation can be easily repeated for $\gamma\gamma \to H \to ZZ$ process below its nominal threshold (the nonresonant background is negligible here). The corresponding cross sections are ~ 50 fb. Therefore, provided the luminosity integral ~ 10 fb^{-1}, one can also observe a Higgs boson in ZZ decay mode in the whole region of M_H considered here. The comparison of Higgs boson couplings with different gauge bosons will be essential test of SM concerning Higgs mechanism of the mass origin.

- If the Higgs boson mass is near 140 GeV, one can hope to observe Higgs boson decays into $b\bar{b}$ and W^+W^-. It provides an opportunity to compare the Higgs boson coupling to quarks and to gauge bosons and in this way to test the Higgs boson origin of particle masses.

4. The discovery potential of photon colliders for new physics

In the table below we present the discovery potential for photon colliders based on e^+e^- colliders with $2E = 0.5$ TeV and for integrated luminosity $\mathcal{L}_{\gamma\gamma}\, dt = 20$ fb^{-1}. The sign * denotes reaction $\gamma\gamma \to P\bar{P}$ for considered particle P.

Particles of SUSY and leptoquarks

particle	$\tilde{W}$	$\tilde{W}$	$\tilde{\ell}$, $H^{\pm}$, $\tilde{q}$	$\tilde{g}$	$\tilde{Z}$	(ℓq)	(ℓt)
reaction	$\gamma e \to \tilde{W}\tilde{\nu}$	*	*	*	$\gamma e \to \tilde{Z}\tilde{e}$	*	$\gamma\gamma \to \bar{t}\bar{\ell}\,(\ell t)$
Mass (TeV)	0.45	0.4	0.2	0.13	0.2	0.2	0.2

Excited leptons and quarks, new Z and W, Dirac–Schwinger monopole $\mathcal{M}$,

particle	e^*	ℓ^*, q^*	Z'	W'	$\mathcal{M}$
reaction	$\gamma e \to e^*$	$\gamma\gamma \to \ell\ell^*$	$e^+e^- \to Z'$	$\gamma e \to \nu W'$	$\gamma\gamma \to \gamma\gamma$
Mass (TeV)	0.45	0.35	0.5	0.3	$5 \div 10$

This work is supported by grants INTAS – 93–1180 ext and RFBR – 96–02–19079.

References

[1] I.F. Ginzburg, G.L. Kotkin, V.G. Serbo and V.I. Telnov, Sov. *ZhETF Pis'ma.* 34 (1981) 514; *Nucl. Instr. and Methods in Physics Research (NIMR)* 205 (1983) 47; I.F. Ginzburg, G.L. Kotkin, S.L. Panfil, V.G. Serbo and V.I. Telnov, *NIMR* 219 (1983) 5.

[2] Zeroth-order Design Report for the NLC, SLAC Report 474 (1996); TESLA, SBLC Conceptual Design Report, DESY (1997) To be published.

[3] G.L. Kotkin, V.G. Serbo, hep-ph /96-11345.

[4] J.F. Gunion, L. Poggiolli and R. van Kooten, Higgs Boson Discovery and Properties, hep-ph/9703330 (1997).

[5] I.F. Ginzburg, G.L. Kotkin, S.L. Panfil and V.G. Serbo, *Nucl. Phys.* **B228** (1983) 285.

[6] I.F. Ginzburg, I.P. Ivanov, hep-ph/9704220.

[7] D.A. Morris, T.N. Truong and D. Zappala, *Phys. Lett.* **B323** (1994) 421.

[8] A.I Vainshtein, M.B. Voloshin, V.I. Zakharov, and M.A. Shifman, *Sov. J. Nucl. Phys.* **30** (1979) 711.

[9] G. Belanger and F. Boudjema, *Phys. Lett.* **B288** (1992) 210.